

## New Encapsulation of Fucoxanthin Isolated from *Cyclotella striata* by Nano Chitosan–Pectin using Ionic Gelation Method

Ridho Nahrowi<sup>1</sup>, Siti Solehati<sup>2</sup>, Widyastuti Widyastuti<sup>2</sup>, Ni Luh Gede Ratna Juliasih<sup>2</sup>, Kamisah Delilawati Pandiangan<sup>2</sup>, Andi Setiawan<sup>2</sup>, John Hendri<sup>2\*</sup>

<sup>1</sup>Doctoral Program Faculty of Mathematics and Science, Lampung University, Bandar Lampung, 35145, Indonesia

<sup>2</sup>Department of Chemistry, Faculty of Mathematics and Science, Lampung University, Bandar Lampung, 35145, Indonesia

\*Corresponding author: john.hendri@fmipa.unila.ac.id

### Abstract

Fucoxanthin is an anticancer, antioxidant, antimicrobial, and anti-inflammatory bioactive compound. Unfortunately, the conjugated double bonds of the fucoxanthin structure make it unstable, posing issues for product development, particularly with regard to shelf life. This research study aims to synthesize nano chitosan–pectin and encapsulate isolated fucoxanthin by nano chitosan–pectin using an ionic gelation method. Fucoxanthin was obtained through isolation of microalgae species *Cyclotella striata*. The best result of nanoparticle size using a particle size analyzer was chitosan:pectin 1 : 2 of 172 nm. Fourier transform infrared analysis showed that there was an interaction between chitosan–pectin and fucoxanthin, which was characterized by a shift in the C=O absorption fucoxanthin from 1736 to 1632 cm<sup>-1</sup>. The result of morphological analysis of nano chitosan–pectin–fucoxanthin using a scanning electron microscope shows a spherical morphology with a size between 140 and 265 nm. The result of encapsulation efficiency was 75.18%, whereas encapsulation stability increased fucoxanthin oxidation half-life 4.7 times longer than that of unencapsulated fucoxanthin. The nano chitosan–pectin could be utilized as a matrix conjugate to increase the stability of fucoxanthin significantly by encapsulation. This information is expected to be useful in developing encapsulation applications for unstable compounds.

### Keywords

Chitosan, Encapsulation, Fucoxanthin, Ionic Gelation, Pectin

Received: 29 January 2024, Accepted: 4 April 2024

<https://doi.org/10.26554/sti.2024.9.3.517-528>

## 1. INTRODUCTION

Fucoxanthin is a marine carotenoid that is currently being developed especially in the pharmaceutical industry (Pajot et al., 2022). This carotenoid is an antimicrobial, anti-inflammatory, antioxidant, and anticancer bioactive compound (Cordenonsi et al., 2019). However, despite its potential health benefits, fucoxanthin is unstable when stored over long periods. The conjugated double bonds in the structure of fucoxanthin make it susceptible to degradation by pH, light, and oxygen (Quan et al., 2013). Previous studies have confirmed the importance of encapsulating fucoxanthin to overcome its instability problem (Oliyaei et al., 2020).

Recently, several researchers have used microalgae as a source of fucoxanthin to develop their studies. Microalgae have been proven to be an excellent bioresource of fucoxanthin due to fast growth and high fucoxanthin content (Pajot et al., 2022). One of the microalgae used as fucoxanthin producer is *Cyclotella* sp. Guo et al. (2016) investigated several types of microalgae as fucoxanthin producer. The result displayed

*Cyclotella cryptica* as a potential fucoxanthin producer due to grow well in several different conditions (Guo et al., 2016). Based on a literature review, this is one of microalgae that have high of biomass concentration and fucoxanthin content (Khaw et al., 2022). However, information regarding another *Cyclotella* species as sources of fucoxanthin production is still scarce. Hence, in this study, we used one of the *Cyclotella* species for the study of fucoxanthin, namely *Cyclotella striata* (*C. striata*).

Numerous conjugate matrices have been successfully used for fucoxanthin encapsulation to enhance the stability of fucoxanthin using ionic gelation method. The network formed through ionic gelation provides stability to the encapsulated material, protecting it from degradation due to environmental factors such as pH, temperature, and mechanical stress (Chun et al., 2014). For example, fucoxanthin encapsulated in chitosan-casein enhances the storage stability of fucoxanthin during four weeks of storage (Koo et al., 2016). Chitosan-glycolipid used to encapsulate fucoxanthin increases the fucoxanthin stability compared to the standard, which is indicated by

an increase in its half-life (Ravi and Baskaran, 2015). However, the addition of tripolyphosphate in the ionic gelation method is very risk for human health. It is associated with an increased risk of coronary artery disease in humans (Sriamornsak and Dass, 2022). This research study aims to synthesize nano chitosan–pectin using an ionic gelation method, by utilizing pectin polyanion as a substitute for tripolyphosphate, and also encapsulate isolated fucoxanthin by nano chitosan–pectin. The novel contribution of this research is the conjugate matrix of nano chitosan–pectin, which was attempted to be designed to encapsulate fucoxanthin using the ionic gelation method. The encapsulation of fucoxanthin in nano chitosan–pectin was hypothesized to enhance the stability of fucoxanthin. The nano chitosan–pectin conjugate matrix had been successfully utilized to encapsulate pelargonidin. This compound was derived from an anthocyanin group that had almost similar biological activity as fucoxanthin (Karim et al., 2022). Nevertheless, the information on fucoxanthin encapsulation via nano chitosan–pectin has yet been carried out.

The biopolymers of chitosan and pectin were widely utilized for the design of new conjugate matrices in biopharmaceutical products (Tian et al., 2020). Chitosan (poly-N-glucosamine) is a natural cationic polymer that has a lot of positively charged free amino groups that enable its reaction with various negatively charged materials to form a polyelectrolyte complex that can be utilized for drug delivery purposes (Salama et al., 2020). Pectin (poly-D-galacturonic acid) is a negatively charged polymer that is widely used in the food industry because of its high availability and non toxicity (Zhao et al., 2020). Chitosan–pectin has succeeded in increasing the stability of quercetin, anthocyanin, and beta-carotene via the encapsulation process (Khan et al., 2021; Xie et al., 2023; Wang et al., 2023).

Based on the above, this study series had been carried out, specifically isolation of fucoxanthin via cultivation, extraction, and purification of *C. striata* microalgae, synthesis of nano chitosan–pectin using the ionic gelation method, and then encapsulation of fucoxanthin dropwise to obtain fucoxanthin encapsulated in nano chitosan–pectin. This study provides a strategy for constructing encapsulation of unstable compounds with different conjugate matrices, which processes potential pharmaceutical applications.

## 2. EXPERIMENTAL SECTION

### 2.1 Biomaterial and Chemicals

The equipment used in this research were glassware, a UV–Vis spectrophotometer (Agilent Technologies Cary 100), Fourier transform infrared (Agilent Technologies Cary 630), a differential scanning calorimeter (DSC) (Hitachi X-DSC 7000), a particle size analyzer (PSA) (Mastersizer, Malvern Panalytical), and a scanning electron microscope (SEM) (Zeiss Evo MA10).

The *C. striata* microalgae were obtained from the collection of the Biochemical Laboratory, Bandung Institute of Technology, Tanjung Bidadari, Thousand Islands. The shrimp shells were collected from free-market Gudang Lelang, Teluk Betung,

Bandar Lampung. CP Kelco provided the pectin ( $C_6H_{10}O_7$ ) (food grade). FUJIFILM Wako Pure Chemical Corporation supplied the standard chitosan  $[C_6H_{11}NO_4]_n$ . Hydrochloric acid (HCl), acetic acid ( $CH_3COOH$ ), sodium hydroxide (NaOH), and ethanol ( $CH_3OH$ ) were from Merck KGaA.

### 2.2 Isolation of Fucoxanthin

Isolation of fucoxanthin from *C. striata* microalgae was carried out through several steps, including cultivation, extraction, and purification. Initially, the stock solution of *C. striata* was cultivated in seawater media for 14 days referring to the modified method of Kusumaningtyas et al. (2017). On the 14<sup>th</sup> day after cultivation, the seawater culture was centrifuged to obtain *C. striata* microalgae biomass. A total of 6.1 g of biomass was extracted by 18 mL of ethanol and then centrifuged to separate extract and waste (Perez et al., 2019). The fucoxanthin extract was purified using medium-pressure liquid chromatography (MPLC). Approximately 1 mL of ethanol extract was injected into the MPLC at a flow rate of 25 mL/min. The sample was then fractionated using  $SiO_2$  as the stationary phase and ethanol as the mobile phase. The detector used was a photodiode array at wavelengths 220, 254, and 364 nm. The MPLC fractions of fucoxanthin were then characterized using a UV–Vis spectrophotometer and stored in a dark bottle.

### 2.3 Extraction of Chitosan

The chitosan extraction was carried out referring to the modified method recognized by Al Hoqani et al. (2020). In the first step, 100 g of shrimp shell was deproteinized by 10% NaOH at 90°C for 2 hours. The deproteinated sample was reacted by 1.25 N HCl for 2 hours at 90°C. Approximately 8.7 g of chitin was deacetylated by 60% of NaOH for 4 hours at 90°C. The sample was washed with distilled water and dried using an oven at 60°C for 18 hours. Chitosan was ready to be used for the synthesis of nano chitosan–pectin.

### 2.4 Synthesis of Nano Chitosan–Pectin

The synthesis of nano chitosan–pectin was carried out using the ionic gelation method that referred to Hafez et al. (2018) report but with modification. In the first step, 200 mg of chitosan was dissolved in 200 mL of 1.5% acetic acid so the concentration was 1 mg/mL. The solution was stirred and sonicated for 1 hour each. A total of 250, 500, and 750 mg pectin were dissolved in 100 mL distilled water respectively so the concentration was 2.5, 5, and 7.5 mL. The solutions were stirred and sonicated for 1 hour each. Next, 20 mL of pectin solution was added to 50 mL of chitosan solution dropwise while stirring constantly for 1 hour. The ratios of chitosan mass:pectin mass were 1:1, 1:2, and 1:3. Samples were stored at –25°C and dried using a freeze dryer. The nano chitosan–pectin with the smallest size was employed for the encapsulation of fucoxanthin.

### 2.5 Encapsulation of Fucoxanthin

Fucoxanthin encapsulation was carried out based on the method described by Koo et al. (2023) but with modification. The fucoxanthin powder was dissolved in ethanol so the concentration

was 200 ppm. A total of 200 mL of nano chitosan–pectin solution was added to 15 mL of 200 ppm fucoxanthin solution dropwise. The process of adding the nano chitosan–pectin solution to the fucoxanthin solution was carried out for 1 hour with constant stirring. The nano chitosan–pectin–fucoxanthin solution was then frozen using a freezer for 40 hours and dried using a freeze dryer. The nano chitosan–pectin–fucoxanthin powder was then analyzed via encapsulation efficiency and stability test.

## 2.6 Encapsulation Efficiency of Fucoxanthin

Analysis of the encapsulation efficiency of fucoxanthin was obtained as a comparison of the mass of encapsulated fucoxanthin with the total mass of fucoxanthin used (Oliyaei et al., 2020). A total of 15 mg of sample was added to 5 mL of ethanol and sonicated for 30 minutes. Approximately 3 mL of sample was taken, and the absorbance was measured using a UV–Vis spectrophotometer at 448 nm. Fucoxanthin concentration was determined based on a standard curve obtained from a standard solution with different concentrations. The encapsulation efficiency was determined based on the Equation (1).

$$EE = \frac{W_R}{W_T} \times 100\% \quad (1)$$

Where EE is the encapsulation efficiency,  $W_R$  is the actual weight of fucoxanthin, and  $W_T$  is the theoretical weight of fucoxanthin.

## 2.7 Stability of Fucoxanthin

The fucoxanthin stability test was carried out using two samples, which were fucoxanthin and nano chitosan–pectin–fucoxanthin. A total of 10 mg fucoxanthin was dissolved in 50 mL of ethanol to obtain a concentration of 200 ppm. The fucoxanthin solution was left at 25°C for 5 days. At certain time intervals, a 3 mL sample was taken, and the absorbance was measured at a wavelength of 350–800 nm. The stability test of nano chitosan–pectin–fucoxanthin was conducted by modifying the Oliyaei et al. (2020) method at room temperature. A total of 50 mg of sample was put into a vial, covered by aluminum foil, and stored for 2 weeks. At certain intervals, a 3 mg sample was taken, and the fucoxanthin concentration was determined as explained in Subsection 2.7. Fucoxanthin degradation was calculated using Equation (2). The oxidation half-life of fucoxanthin was calculated via Equation (3).

$$n_T = \frac{W_T}{W_0} \times 100\% \quad (2)$$

$$N_t = N_0 \left( \frac{1}{2} \right)^{\frac{t}{t_{1/2}}} \quad (3)$$

where  $n_T$  is the concentration of fucoxanthin at a certain time,  $W_T$  is the weight of fucoxanthin at a certain time,  $W_0$  is the initial weight of fucoxanthin,  $N_t$  is the amount of final fucoxanthin,  $N_0$  is the amount of initial fucoxanthin,  $t$  is time of degradation, and  $t_{1/2}$  is half-life of fucoxanthin oxidation.

## 2.8 Characterizations

The polymer functional groups were analyzed via Fourier transform infrared (FTIR) (Agilent Technologies Cary 630) in the range of 4000–700  $\text{cm}^{-1}$ . The thermal properties of extracted and standard chitosans were measured using a DSC (Hitachi X-DSC 7000). The particle size distribution of nano chitosan–pectin was characterized using a laser scattering PSA (Mastersizer, Malvern Panalytical). The surface morphology of nano chitosan–pectin and nano chitosan–pectin–fucoxanthin was examined using an SEM (Zeiss Evo MA10).

## 3. RESULTS AND DISCUSSION

### 3.1 Isolation of Fucoxanthin

The *C. striata* microalgae were collected from Tanjung Bidadari, Thousand Island, Indonesia. Microalgae were considered a promising and sustainable fucoxanthin bioresource owing to their high fucoxanthin and superior growth rates (Khaw et al., 2022). The microalgae of the genus *Cyclotella* have been proven to be useful as a bioresource for marine-based fucoxanthin production due to high of biomass concentration and fucoxanthin content. Table 1 presents literature review regarding biomass concentration and fucoxanthin content in microalgae.

In Table 1, *Cyclotella cryptica* has highest of biomass concentration and fucoxanthin content compared to other microalgae. We hypothesized that other species of *Cyclotella* sp. have potential as fucoxanthin producers based on biomass concentration and fucoxanthin content. In consequence, we used *C. striata* as the fucoxanthin bioresource. In this study, 1 g (wet weight) of microalgae produced 2 mg of fucoxanthin. Nevertheless, further studies on the biomass concentration and fucoxanthin content of *C. striata* are still needed to complete this study. Figure 1 presents the *C. striata* culture in seawater.

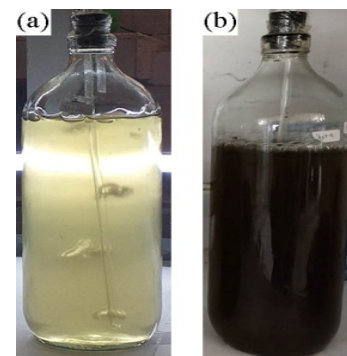


Figure 1. *C. striata* Culture at (a) Day 1<sup>st</sup> and (b) Day 14<sup>th</sup>

In Figure 1, an increase in culture color density between Days 1<sup>st</sup> and 14<sup>th</sup> can be observed, which indicates an increase in microalgae cell number. The cell growth rate is affected by temperature, salinity or salt content,  $\text{CO}_2$  levels, carbohydrates, proteins, and fats (Gatamaneni et al., 2018). On the 14<sup>th</sup> day after cultivation, *C. striata* microalgae were harvested. Day 14 is the stationary phase of *Cyclotella* sp. growth (Cupo et al., 2021). This phase is the optimum condition for harvesting

**Table 1.** Biomassa Concentration and Fucoxanthin Content in Microalgae (Khaw et al., 2022)

Microalgae	BC (g/L)*	Fx C (% DW)**	References
<i>Cyclotella cryptica</i>	1.72	1.29	(Guo et al., 2016)
<i>Pavlova</i> sp.	0.92	0.26	(Kanamoto et al., 2021)
<i>P. tricornutum</i>	1.56	0.75	(Wang et al., 2018)
<i>Cylindrotheca fusiformis</i>	1.64	1.58	(Wang et al., 2018)
<i>Sellaphora minima</i>	1.71	0.75	(Gérin et al., 2020)

\* BC is biomass concentration

\*\* Fx C is fucoxanthin conten (% dry weight)

microalgae because the cell density is higher than that in other phases (Rahman et al., 2020). The extract of fucoxanthin was purified via MPLC. MPLC is a preparative chromatography, meaning that this instrument is used to separate specific component effectively from complex compounds. In principle, the stationary phase of MPLC column interacts selectively with the target compound. Separation of the target compound occurs when the extract is eluted into the stationary phase by the mobile phase. After eluting, all fractions in the extract were detected, and the target compound was collected for further analysis (Primdahl et al., 2022). Figure 2 presents the MPLC chromatogram of fucoxanthin extract.

In Figure 2, the MPLC chromatogram showed that there were four peaks in fractions 8–11 which caused by the carotenoid components in the ethanol extract, one of them was fucoxanthin which probably found in fractions 8–9. The four fractions were separated in different tubes and then analyzed using a UV–Vis spectrophotometer to determine its maximum wavelength as a specific characteristic for the absorption of fucoxanthin. The UV–Vis analysis provides information about the electronic excitation states of molecules and is useful for determining the fucoxanthin structure based on maximum wavelength (Amekura, 2018) because of its simplicity, sensitivity, reliability, and low cost (Passos and Saraiva, 2019). Figure 3 presents the UV–Vis spectra of MPLC fractions in Tubes 8–11.

Based on Figure 3, the UV–Vis spectra resulting from the fractionation of ethanol extract using MPLC show differences in maximum wavelength, except that Tubes 8 and 9 have a similar pattern and maximum wavelength peak, namely, 448 nm. Figure 3 also shows that the carotenoid compounds in Tubes 10 and 11 have two maximum wavelengths, specifically 416 and 448 in Tube 10 and 408 and 448 in Tube 11. The compounds contained in Tubes 10 and 11 indicated viloxanthin and neoxanthin (Ashenafi et al., 2023). A sight maximum wavelength peak above 650 nm indicates the presence of chlorophyll compounds in the four fractions.

The fucoxanthin has UV–Vis absorption characteristics at a maximum wavelength of 448 (Sabdono et al., 2021; Singh et al., 2022). This maximum wavelength originated from nine conjugated double bonds, 10 alkyl substituents, and one exo double bond. The fucoxanthin of this research may be found in Tubes 8 and 9 with a maximum wavelength of 448 nm. These

results confirm the previous hypothesis that the fucoxanthin compound was found in fractions 8–9. The compounds contained in Tubes 8 and 9 are then collected and used for the encapsulation process.

### 3.2 Extraction of Chitosan

Chemical extraction of chitosan from shrimp shells through at least three stages, specifically deproteination, demineralization, and deacetylation. The deproteination reaction using an alkaline solution can break or damage the chemical bonds between chitin and protein. This procedure is an important stage of polysaccharide purification such as chitin. In the next stage, the minerals in chitin such as calcium carbonate and magnesium carbonate are decomposed using strong acid to become calcium chloride or magnesium chloride and emit carbon dioxide. At the last stage, an alkaline hydrolysis process is carried out to remove the acetyl group of the chitin monomer in order to generate chitosan (Santos et al., 2020).

The chitin yield obtained was 21.93%. After the deacetylation process, chitosan produced a yield of 17.74%. Theoretically, the chitin content in shrimp shells is approximately 20–30%. Chitin extraction from shrimp shells in Cuddalore and Annankovil water in India was 22.42% (Arulmoorthy et al., 2022). The chitin yield resulting from this research was 21.93%, which was almost similar to the results that have been reported by Arulmoorthy et al. (2022).

To determine the functional groups and deacetylation degree of chitosan, the FTIR was employed. Figure 4 presents the FTIR spectrum of these compounds. The FTIR absorption of extracted chitosan (Figure 4a) indicated that of hydrogen (OH) stretching vibration, CH stretching vibration, and amide I bonds were observed at 3287, 2870, and 1647  $\text{cm}^{-1}$ , respectively. The standard chitosan (Figure 4b) showed absorption peaks at 3287, 1647, and 1580  $\text{cm}^{-1}$ , respectively, indicating the presence of hydrogen bonds (OH), amide I bonds (C=O), and amide II bonds (NH). The results of the FTIR analysis showed that chitosan had a similar pattern as standard chitosan.

The important parameter to determine the quality of chitosan is the deacetylation degree. The deacetylation degree describes the number of free amino groups in chitosan as a polysaccharide or the amount of chitin acetyl groups that are removed to turn into chitosan (Hosney et al., 2022). The deacetylation degree of chitosan was determined based on the

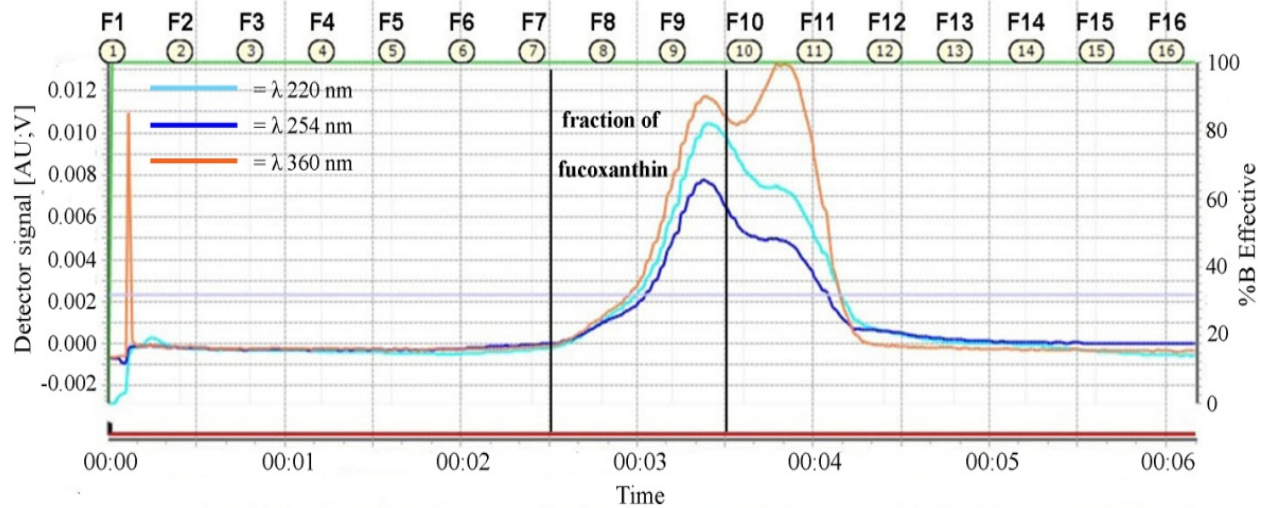


Figure 2. MPLC Chromatogram of Fucoxanthin Extract.

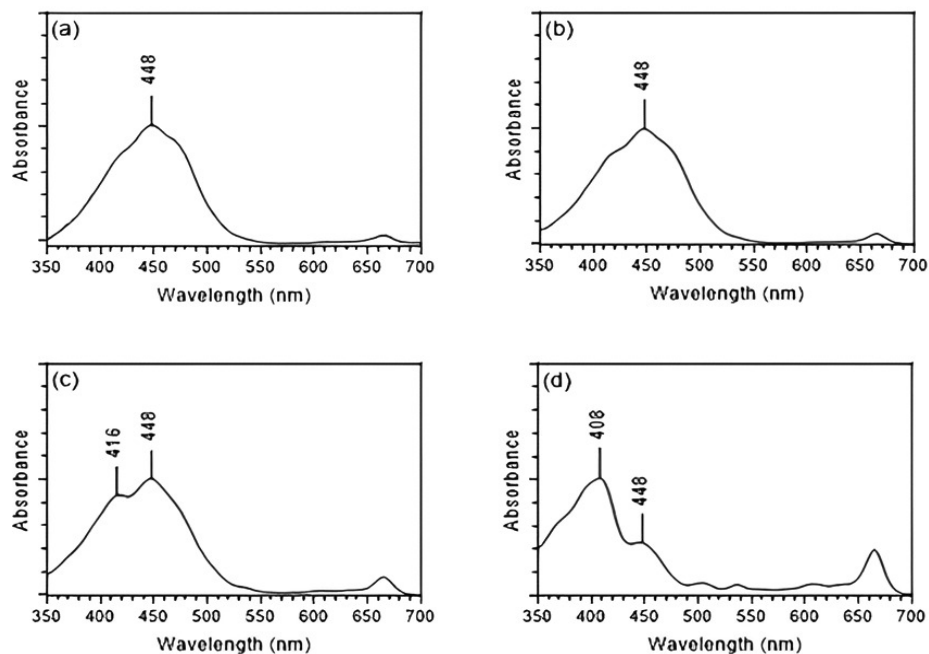


Figure 3. UV-Vis Spectra of MPLC Fraction in (a) Tube 8, (b) Tube 9, (c) Tube 10, and (d) Tube 11

ratio of amide III absorbance at  $1320\text{ cm}^{-1}$  to the amide II absorbance at  $1420\text{ cm}^{-1}$ . The deacetylation degree of extracted chitosan is slightly higher than standard chitosan. The deacetylation degree of extracted chitosan was 80.06%, whereas that of standard chitosan was 79.96%. This result was also reinforced by the observation that the amide I intensity of extracted chitosan was smaller than that of standard chitosan. In other words, the number of free amine groups in extracted chitosan is greater than that in standard chitosan. These results indicate the efficiency of removing the acetyl group, which reflects the

chitosan purity.

The DSC analysis is employed to determine the thermal analysis of chitosan. Figure 5 presents the DSC curves.

The extracted chitosan (Figure 5a) had endothermic and exothermic peaks at  $85^{\circ}\text{C}$  and  $307^{\circ}\text{C}$ , respectively. The endothermic and exothermic peaks of standard chitosan (Figure 5b) were  $68^{\circ}\text{C}$  and  $295^{\circ}\text{C}$ , respectively. The endothermic peak of both chitosan was associated with water evaporation, whereas the exothermic peaks were related to chitosan decomposition (Corazzari et al., 2015). The extracted chitosan had a broader

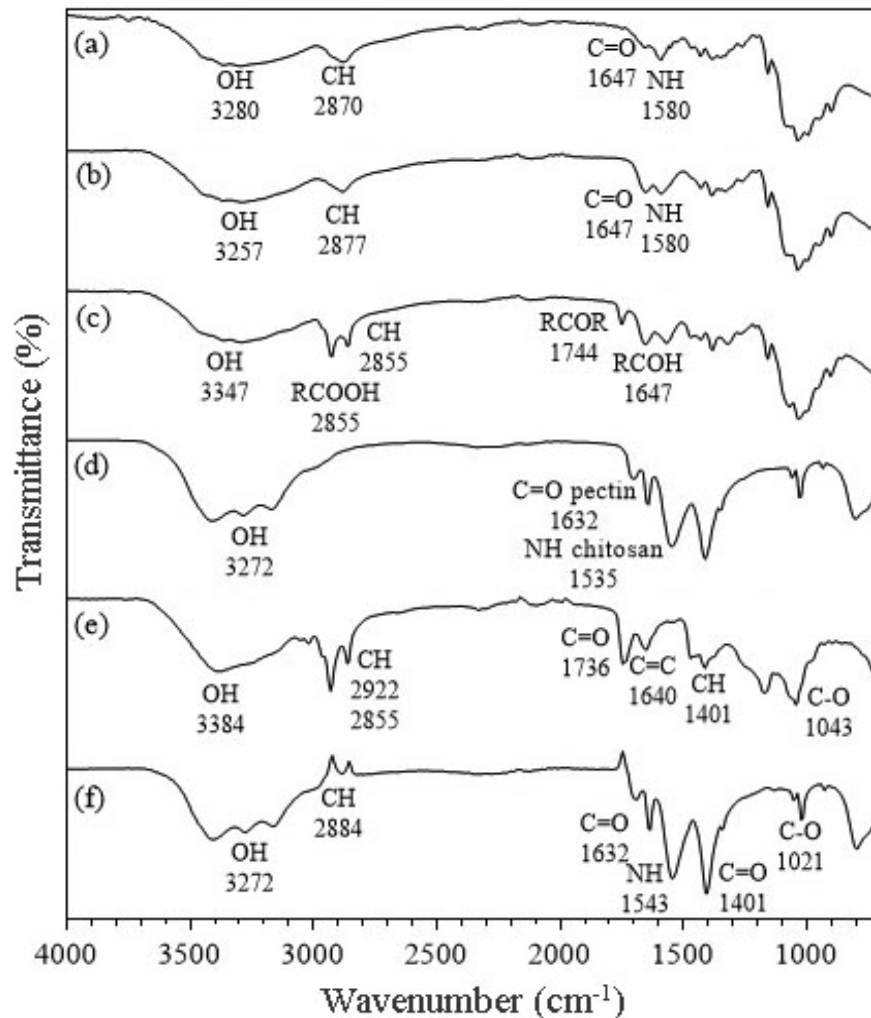


**Figure 4.** FTIR Spectrum of (a) Extracted Chitosan, (b) Standard Chitosan, (c) Pectin, (d) Nano Chitosan–Pectin, (e) Fucoxanthin, and (f) Nano Chitosan–Pectin–Fucoxanthin.

endothermic area than standard chitosan. This is because extracted chitosan had additional free amino residues, so it had a higher water-holding capacity and the interaction of hydrogen with water molecules was stronger. The results of this DSC analysis have confirmed the validity of the FTIR analysis, that the amide II intensity of extracted chitosan was greater than amide I. A lot of free amino residues are a crucial factor for encapsulation stability. The free amino residues as an active site of chitosan attract negatively compound, leading to higher encapsulation efficiency. It also improves the ionic character of chitosan, so improve the interaction between chitosan with encapsulated compound. This will enhance the the stability of encapsulated compound (Kang et al., 2022; Negi and Kesari, 2022).

### 3.3 Synthesis of Nano Chitosan–Pectin

The synthesis of nano chitosan–pectin was conducted using the ionic gelation method, referring to the research reported by Hafez et al. (2018). This research employed pectin polyanion as a substitute for sodium tripolyphosphate, which was added dropwise to the chitosan solution. Figure 6 presents the particle size distribution of chitosan–pectin and nano chitosan–pectin.

As shown in Figure 6, the difference in particle size distribution of the chitosan and pectin solutions before and after mixing can be observed. Chitosan (Figure 6a) and pectin (Figure 6b) have a particle size distribution between 1000 and 4000 nm, respectively. The size distributions of nano chitosan–pectin (Figures 6c–6g) with a ratio of 1:2, 2:1, 1:3, 3:1, and 1:1 were 122–255 nm, 255–955 nm, 530–2670 nm, 78–1480 nm, and 255–3580 nm, respectively.

The nano chitosan–pectin that has the smallest particle size can be seen in the ratio of chitosan:pectin of 1:2 with an aver-

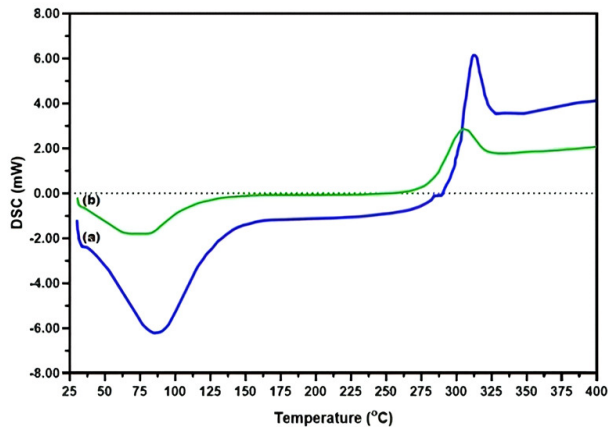


**Figure 5.** DSC Curves of (a) Extracted Isolated Chitosan and (b) Standard Chitosan.

age particle size of 172 nm. There is a very clear relationship between the percentage of raw materials used and the size of particles produced. Increasing the amount of pectin causes an increase in the particle size of nano chitosan–pectin produced. The increase in the percentage of chitosan used is also comparable to the increase in the size of nano chitosan–pectin (Salama et al., 2020). The stoichiometry of the complexation reaction of amino groups with pectin carboxylate groups greatly influences the resulting nanoparticle size. The advantage of using nano chitosan–pectin as an encapsulation matrix includes provides stability, high biocompatibility, and non-toxicity, making it suitable for encapsulation applications (Rebitski et al., 2020; Călinoiu et al., 2019).

The absorption peaks at 3347, 2922, and 2855  $\text{cm}^{-1}$  respectively indicated OH alcohol, OH carboxyl, and CH aliphatic of pectin (Figure 4c). The stretching vibrations of C=O ester and C=O carboxylate pectin were shown by absorption peaks at 1744 and 1647  $\text{cm}^{-1}$ , respectively. The absorption peak of nano chitosan–pectin (Figure 4d) at 3272  $\text{cm}^{-1}$  indicated OH alcohol. The presence of a glycosidic bond absorption peak at 1021  $\text{cm}^{-1}$  indicated that after chitosan and pectin reacted, no depolymerization of the two polymers occurred, leaving only the monomers. The absorption peaks observed at 1632 and 1535  $\text{cm}^{-1}$  indicated the vibration of the pectin carbonyl and chitosan amine. The shift in the wave number indicates that there is an environmental change in the two groups, which originates from the ionic interaction and hydrogen bond between chitosan with pectin (Safitri et al., 2022). The hydrogen bond causes weak carbonyl bending, which is confirmed by the absorption peak at 1692  $\text{cm}^{-1}$  (Tian et al., 2020). This interaction is confirmed by the shift of peak at 3384 to 3272  $\text{cm}^{-1}$  (Jamshidzadeh et al., 2020). Figure 7 presents the SEM images of nano chitosan–pectin and nano chitosan–pectin–fucoxanthin.

The surface morphology observed on nano chitosan–pectin (Figure 7a) was spherical, with a diameter of 150–200 nm.

Jabbari et al. (2020) have reported the results of the nano chitosan synthesis using the ionic gelation method. The results of surface morphology analysis showed that the resulting nano chitosan also had spherical morphology. Chitosan polymer had a basic structure of glucose, which was dominated by OH groups. The presence of this group caused very strong intramolecular or intermolecular hydrogen bonds. The addition of pectin polyanions to the chitosan polymer will cause damage to intermolecular hydrogen bonds and bind to pectin, thereby reducing the size of chitosan particles.

### 3.4 Encapsulation of Fucoxanthin

Based on the spectrum of fucoxanthin (Figure 4e), the existence of the ketone group was observed at 1736  $\text{cm}^{-1}$ . The existence of alkane groups (CH) was observed at 2922 and 2825  $\text{cm}^{-1}$ . Absorption at 3384  $\text{cm}^{-1}$  indicated OH vibrations. The FTIR spectrum of nano chitosan–pectin–fucoxanthin (Figure 4f) showed the CH stretching vibration of alkane at 2884  $\text{cm}^{-1}$ . The absorption peak at 1632  $\text{cm}^{-1}$  indicated C=O acetate and C=O conjugate. The OH group was observed at 3272  $\text{cm}^{-1}$ . The C–O and C=C trans absorption peaks were observed at 1021 and 797  $\text{cm}^{-1}$ , respectively. The main difference between the FTIR spectrum of fucoxanthin and nano chitosan–pectin–fucoxanthin was the shift in C=O absorption from 1736 to 1632  $\text{cm}^{-1}$ . This shift was caused by hydrogen bonds and electrostatic interactions in nano chitosan–pectin (Koo et al., 2023). High humidity levels may interfere with infrared absorption thereby reducing allene intensity (Oliyaei et al., 2020). The FTIR spectrum results above indicated that the fucoxanthin compound had been successfully encapsulated in nano chitosan–pectin. Figure 7b shows that the nano chitosan–pectin–fucoxanthin also had a spherical morphology. The figure also shows the existence of agglomeration in the nanocapsule. The FTIR spectrum results above indicated that the fucoxanthin compound had been successfully encapsulated in nano chitosan–pectin. According to a study conducted by Quiñones et al. (2018) the encapsulation process can produce matrix agglomeration. Considering this, a further study was carried out using SEM, as seen in Figures 7a and 7b. This agglomeration process was due to as long as encapsulation, the chitosan–pectin nanoparticles move randomly and hydrogen interactions occur between the nanoparticles. For this reason, further study is needed to avoid agglomeration.

To determine the amount of fucoxanthin entrapped in the nano chitosan–pectin core, encapsulation efficiency analysis was conducted. The analysis was based on research by Oliyaei et al. (2020) who used a UV–Vis spectrophotometer. The encapsulation efficiency generated in this research was 75.18%. This fairly large efficiency value indicated that the polyelectrolyte complex structure of the nano chitosan–pectin had very good absorption capacity; thus, fucoxanthin was indeed entrapped in the polyelectrolyte complex. The high lipophilicity of fucoxanthin also facilitated the encapsulation of fucoxanthin in nano chitosan–pectin (Cordenonsi et al., 2019).

The high encapsulation efficiency of this study also was

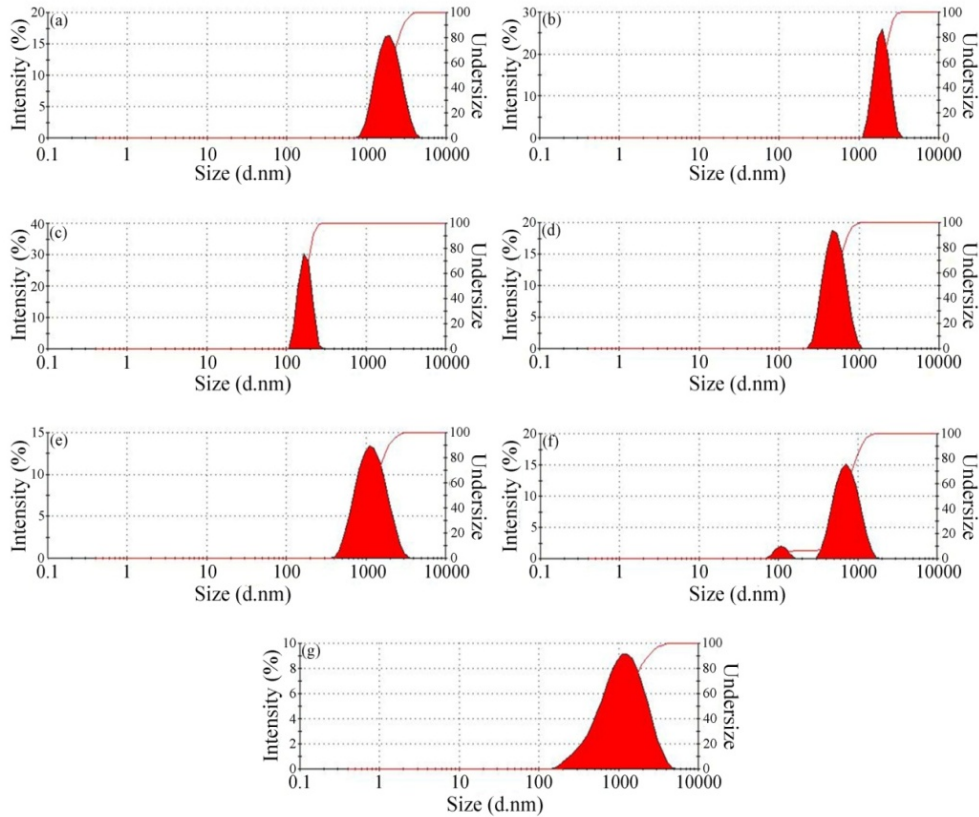


**Figure 6.** Particle Size Distribution of (a) Chitosan, (b) Pectin, (c) Nano Chitosan–Pectin 1:2, (d) Nano Chitosan–Pectin 2:1, (e) Nano Chitosan–Pectin 1:3, (f) Nano Chitosan–Pectin 3:1, and (g) Nano Chitosan–Pectin 1:1

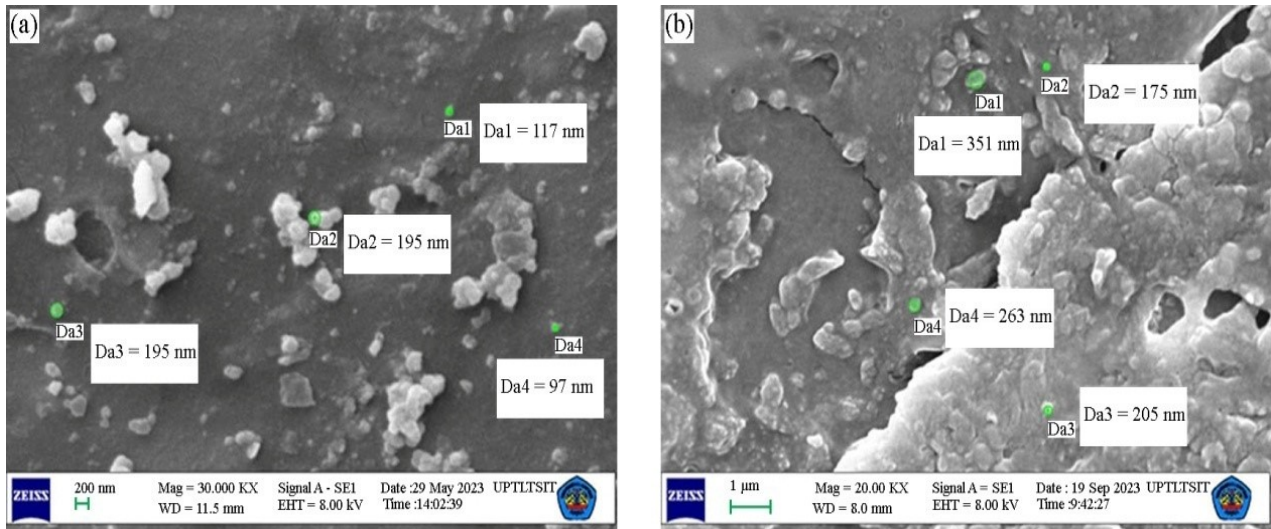


**Figure 7.** SEM Images of (a) Nano Chitosan–Pectin and (b) Nano Chitosan–Pectin–Fucoxanthin

affected by the small size of nano chitosan–pectin. The large nano chitosan–pectin surface area provides more opportunity for its interaction with fucoxanthin (Maciel et al., 2017). The

small particle size has a good uniform distribution, which reduces the likelihood of encapsulated material being localized in certain areas (Mundargi et al., 2016). The high encapsula-

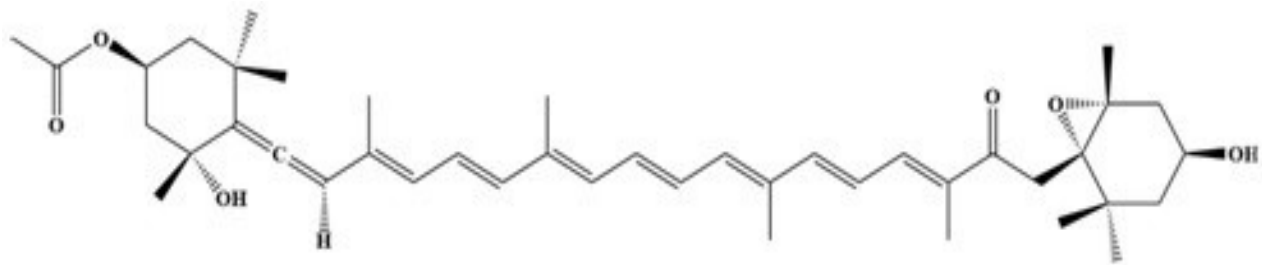


Figure 8. Structure of Fucoxanthin (Ravi and Baskaran, 2015)

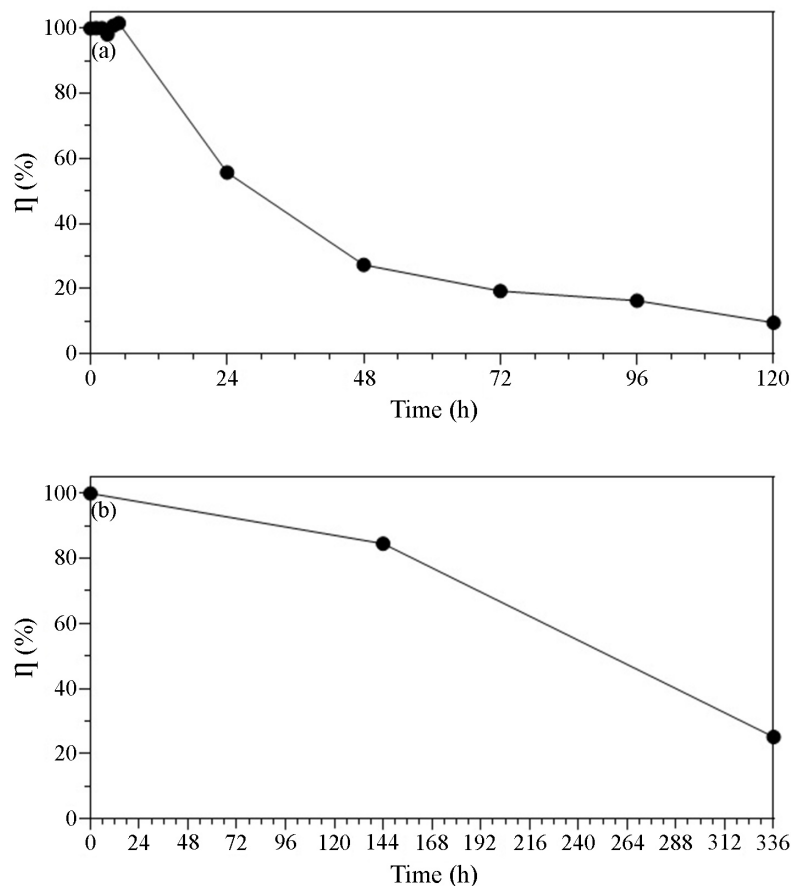


Figure 9. (a) Fucoxanthin Stability in Ethanol and (b) Nano Chitosan-Pectin-Fucoxanthin Stability at Room Temperature in Dark Conditions

tion efficiency also was supported by the stability effect of the small particle size during the encapsulation process (Soukoulis and Bohn, 2018). In conclusion, the novel conjugate matrix nano chitosan-pectin was a very good matrix as a fucoxanthin encapsulation material. Figure 8 presents the structure of fucoxanthin.

The fucoxanthin stability testing was carried out using two samples, namely, fucoxanthin and nano chitosan-pectin-fucoxanthin. Figure 9 presents the results of the fucoxanthin stability

test.

The results of the fucoxanthin test (Figure 9a) showed that the absorbance value of fucoxanthin was stable for up to 6 h. Afterward, the absorbance value of fucoxanthin began to decrease until it remained 10.87% after 5 days of storage. In Figure 8, the fucoxanthin structure has nine conjugated double bonds, which make it susceptible to degradation by oxidation, isomerization, photochemical, or enzymatic reactions (Zhao et al., 2019). Results of the fucoxanthin stability analysis pro-

vide information that degradation of the fucoxanthin structure started to occur after 6 hours of storage. This information was used as a reference for the duration of the fucoxanthin encapsulation process. In this study, the time used for encapsulation of fucoxanthin was 1 h. During the encapsulation process, it was ensured that there was no reduction in fucoxanthin concentration; hence, the encapsulation process ran effectively and efficiently.

Figure 9 shows the difference in the storage stability of fucoxanthin before and after encapsulation. The concentration of fucoxanthin after 5 days of storage was 10.87%, whereas the concentration of fucoxanthin in nano chitosan–pectin after 14 days of storage was 26.32%. The slight decrease in fucoxanthin concentration within 6 days was probably caused by residual unencapsulated fucoxanthin. After 6 days the fucoxanthin was released in the nano chitosan–pectin up to 14 days remaining 26.32%. The small size of nano chitosan–pectin generates a higher surface area to volume ratio, leading to faster release rates of fucoxanthin when compared to larger nanocapsules (Sarma et al., 2022). Nevertheless, additional studies are needed to determine the effect of particle size on the release of fucoxanthin. Based on the calculation of oxidation half-life, the degradation half-life of fucoxanthin was 1.56 days, whereas the degradation of fucoxanthin in nano chitosan–pectin was 7.37 days. These results indicated that the encapsulation process could stabilize fucoxanthin during storage. The network structure of nano chitosan–pectin obstructs the opening of nano chitosan–pectin core to protect conjugated double bonds of fucoxanthin from being oxidized as explained previously (Jamshidzadeh et al., 2020). The novel conjugate matrix nano chitosan–pectin was successful in increasing the stability of fucoxanthin and increasing its oxidation half-life 4.7 times longer than that of unencapsulated fucoxanthin.

#### 4. CONCLUSIONS

In this study, encapsulation of fucoxanthin in nano chitosan–pectin was successfully carried out. The nano chitosan–pectin used to encapsulate fucoxanthin had a particle size of 172 nm. Based on the result of FTIR analysis, a shift in the C=O absorption of fucoxanthin from 1736 to 1632  $\text{cm}^{-1}$  showed the influence of nano chitosan–pectin on the nanocapsule produced. Based on the result of the efficiency analysis, the nanocapsule encapsulation efficiency was 75.18%. The high encapsulation efficiency value indicated that nano chitosan–pectin was suitable for use to encapsulate fucoxanthin. The encapsulation process increases the oxidation half-life of fucoxanthin by 4.7 times longer than that of unencapsulated fucoxanthin. This novel information is very important to be used in further research on the development of the stability of encapsulated antioxidant compounds.

#### 5. ACKNOWLEDGMENT

The author would like to thank the Directorate General of Higher Education, Research and Technology, Ministry of Ed-

ucation, Culture, Research and Technology of the Republic of Indonesia, for the Innovation Research Scheme and Domestic Cooperation funding. The author also thanks the Technical Service Unit, Integrated Laboratory of Innovation and Technology Center (UPT LTSIT), University of Lampung, for providing scanning electron microscope facilities. The author also would like to thank the incorporated company DiethelmKellerSiberHegner (DKSH) Indonesia for providing particle size analyzer facilities.

#### REFERENCES

- Al Hoqani, H. A. S., A. S. Noura, M. A. Hossain, and M. A. Al Sibani (2020). Isolation and Optimization of the Method for Industrial Production of Chitin and Chitosan from Omani Shrimp Shell. *Carbohydrate Research*, **492**(June); 108001
- Amekura, H. (2018). *Compendium of Surface and Interface Analysis*, chapter Ultraviolet-Visible Spectrophotometry. Springer, pages 791–799
- Arulmoorthy, M., G. Anbarasi, M. Srinivasan, and B. Vishnupriya (2022). Biosynthesis and Characterization of Chitosan Based Hydrogel: A Potential *In vitro* Wound Healing Agent. *Materials Today: Proceedings*, **48**(Part 2); 263–275
- Ashenafi, E. L., M. C. Nyman, J. T. Shelley, and N. S. Mattson (2023). Spectral Properties and Stability of Selected Carotenoid and Chlorophyll Compounds in Different Solvent Systems. *Food Chemistry Advances*, **2**(October); 100178
- Călinoiu, L. F., B. E. Ștefănescu, I. D. Pop, L. Muntean, and D. C. Vodnar (2019). Chitosan Coating Applications in Probiotic Microencapsulation. *Coatings*, **9**(3); 194
- Chun, H., C. H. Kim, and Y. H. Cho (2014). Microencapsulation of Lactobacillus Plantarum DKL 109 Using External Ionic Gelation Method. *Korean Journal for Food Science of Animal Resources*, **34**(5); 692
- Corazzari, I., R. Nisticò, F. Turci, M. G. Faga, F. Franzoso, S. Tabasso, and G. Magnacca (2015). Advanced Physico-Chemical Characterization of Chitosan by Means of TGA Coupled On-Line with FTIR and GCMS: Thermal Degradation and Water Adsorption Capacity. *Polymer Degradation and Stability*, **112**(February); 1–9
- Cordenonsi, L. M., A. Faccendini, M. Catanzaro, M. C. Bonferoni, S. Rossi, L. Malavasi, R. P. Raffin, E. E. S. Schapoval, C. Lanni, and G. Sandri (2019). The Role of Chitosan As Coating Material for Nanostructured Lipid Carriers for Skin Delivery of Fucoxanthin. *International Journal of Pharmaceutics*, **567**(August); 118487
- Cupo, A., S. Landi, S. Morra, G. Nuzzo, C. Gallo, E. Manzo, A. Fontana, and G. d'Ippolito (2021). Autotrophic Vs. Heterotrophic Cultivation of the Marine Diatom *Cyclotella cryptica* for Epa Production. *Marine Drugs*, **19**(7); 355
- Gatamaneni, B. L., V. Orsat, and M. Lefsrud (2018). Factors Affecting Growth of Various Microalgal Species. *Environmental Engineering Science*, **35**(10); 1037–1048
- Gérin, S., T. Delhez, A. Corato, C. Remacle, and F. Franck (2020). A Novel Culture Medium for Freshwater Diatoms

- Promotes Efficient Photoautotrophic Batch Production of Biomass, Fucoxanthin, and Eicosapentaenoic Acid. *Journal of Applied Phycology*, **32**(April); 1581–1596
- Guo, B., B. Liu, B. Yang, P. Sun, X. Lu, J. Liu, and F. Chen (2016). Screening of Diatom Strains and Characterization of *Cyclotella cryptica* As a Potential Fucoxanthin Producer. *Marine Drugs*, **14**(7); 125
- Hafez, A. S. M., R. M. Hathout, and O. A. Sammour (2018). Tracking the Transdermal Penetration Pathways of Optimized Curcumin-Loaded Chitosan Nanoparticles Via Confocal Laser Scanning Microscopy. *International journal of biological macromolecules*, **108**; 753–764
- Hosney, A., S. Ullah, and K. Barčauskaitė (2022). A Review of the Chemical Extraction of Chitosan from Shrimp Wastes and Prediction of Factors Affecting Chitosan Yield by Using an Artificial Neural Network. *Marine Drugs*, **20**(11); 675
- Jabbari, N., Z. Eftekhari, N. H. Roodbari, and K. Parivar (2020). Evaluation of Encapsulated Eugenol by Chitosan Nanoparticles on the Aggressive Model of Rheumatoid Arthritis. *International Immunopharmacology*, **85**(August); 106554
- Jamshidzadeh, F., A. Mohebbi, and M. Abdouss (2020). Three-ly Biocompatible pH-Responsive Nanocarriers Based on HNT Sandwiched by Chitosan/Pectin Layers for Controlled Release of Phenytoin Sodium. *International Journal of Biological Macromolecules*, **150**(May); 336–343
- Kanamoto, A., Y. Kato, E. Yoshida, T. Hasunuma, and A. Kondo (2021). Development of a Method for Fucoxanthin Production Using the Haptophyte Marine Microalga *Pavlova* Sp. OPMS 30543. *Marine Biotechnology*, **23**(March); 331–341
- Kang, B. R., J. S. Park, G. R. Ryu, W. J. Jung, J. S. Choi, and H. M. Shin (2022). Effect of Chitosan Coating for Efficient Encapsulation and Improved Stability under Loading Preparation and Storage Conditions of *Bacillus* Lipopeptides. *Nanomaterials*, **12**(23); 4189
- Karim, N., M. R. I. Shishir, Y. Li, O. Y. Zineb, J. Mo, J. Tangpong, and W. Chen (2022). Pelargonidin-3-O-Glucoside Encapsulated Pectin-Chitosan-Nanoliposomes Recovers Palmitic Acid-Induced Hepatocytes Injury. *Antioxidants*, **11**(4); 623
- Khan, M. A., C. Zhou, P. Zheng, M. Zhao, and L. Liang (2021). Improving Physicochemical Stability of Quercetin-Loaded Hollow Zein Particles with Chitosan/pectin Complex Coating. *Antioxidants*, **10**(9); 1476
- Khaw, Y. S., F. M. Yusoff, H. T. Tan, N. A. I. Noor Mazli, M. F. Nazarudin, N. A. Shaharuddin, A. R. Omar, and K. Takahashi (2022). Fucoxanthin Production of Microalgae under Different Culture Factors: A Systematic Review. *Marine Drugs*, **20**(10); 592
- Koo, S. Y., K. T. Hwang, S. Hwang, K. Y. Choi, Y. J. Park, J. H. Choi, T. Q. Truong, and S. M. Kim (2023). Nanocapsulation Enhances the Bioavailability of Fucoxanthin in Microalga *Phaeodactylum tricornerutum* Extract. *Food Chemistry*, **403**(1); 134348
- Koo, S. Y., I.-K. Mok, C.-H. Pan, and S. M. Kim (2016). Preparation of Fucoxanthin-Loaded Nanoparticles Composed of Casein and Chitosan with Improved Fucoxanthin Bioavailability. *Journal of Agricultural and Food Chemistry*, **64**(49); 9428–9435
- Kusumaningtyas, P., S. Nurbaiti, G. Suantika, M. B. Amran, and Z. Nurachman (2017). Enhanced Oil Production by the Tropical Marine Diatom *Thalassiosira* Sp. Cultivated in Outdoor Photobioreactors. *Applied Biochemistry and Biotechnology*, **182**; 1605–1618
- Maciel, V. B., C. M. Yoshida, S. M. Pereira, F. M. Goycoolea, and T. T. Franco (2017). Electrostatic Self-Assembled Chitosan-Pectin Nano- and Microparticles for Insulin Delivery. *Molecules*, **22**(10); 1707
- Mundargi, R. C., M. G. Potroz, S. Park, J. H. Park, H. Shirahama, J. H. Lee, J. Seo, and N. J. Cho (2016). Lycopodium Spores: A Naturally Manufactured, Superrobust Biomaterial for Drug Delivery. *Advanced Functional Materials*, **26**(4); 487–497
- Negi, A. and K. K. Kesari (2022). Chitosan Nanoparticle Encapsulation of Antibacterial Essential Oils. *Micromachines*, **13**(8); 1265
- Oliyaei, N., M. Moosavi Nasab, A. M. Tamaddon, and M. Fazaeli (2020). Encapsulation of Fucoxanthin in Binary Matrices of Porous Starch and Halloysite. *Food Hydrocolloids*, **100**(March); 105458
- Pajot, A., G. Hao Huynh, L. Picot, L. Marchal, and E. Nicolau (2022). Fucoxanthin from Algae to Human, an Extraordinary Bioresource: Insights and Advances in up and Downstream Processes. *Marine Drugs*, **20**(4); 222
- Passos, M. L. and M. L. M. Saraiva (2019). Detection in UV-Visible Spectrophotometry: Detectors, Detection Systems, and Detection Strategies. *Measurement*, **135**(March); 896–904
- Perez, E. B. M., M. C. Ruiz Dominguez, J. E. Morales, and P. C. Mezquita (2019). Fucoxanthin from Marine Microalga *Isochrysis Galbana*: Optimization of Extraction Methods with Organic Solvents. *DYNA*, **86**(210); 174
- Primdahl, K. G., F. A. Hansen, E. J. Solum, J. M. J. Nolsøe, and M. Aursnes (2022). Introduction to Preparative Chromatography: Description of a Setup with Continuous Detection. *Journal of Chemical Education*, **99**(6); 2372–2377
- Quan, J., S. M. Kim, C. H. Pan, and D. Chung (2013). Characterization of Fucoxanthin-Loaded Microspheres Composed of Cetyl Palmitate-Based Solid Lipid Core and Fish Gelatin-Gum Arabic Coacervate Shell. *Food Research International*, **50**(1); 31–37
- Quiñones, J. P., H. Peniche, and C. Peniche (2018). Chitosan Based Self-Assembled Nanoparticles in Drug Delivery. *Polymers*, **10**(3); 235
- Rahman, N. A., T. Katayama, M. E. A. Wahid, N. A. Kasan, H. Khatoon, Y. Yamada, and K. Takahashi (2020). Taxon and Growth Phase-Specific Antioxidant Production by Chlorophyte, Bacillariophyte, and Haptophyte Strains Isolated from Tropical Waters. *Frontiers in Bioengineering and*

- Biotechnology*, **8**(November); 581628
- Ravi, H. and V. Baskaran (2015). Biodegradable Chitosan-Glycolipid Hybrid Nanogels: A Novel Approach to Encapsulate Fucoxanthin for Improved Stability and Bioavailability. *Food Hydrocolloids*, **43**(January); 717–725
- Rebitski, E. P., M. Darder, R. Carraro, P. Aranda, and E. Ruiz Hitzky (2020). Chitosan and Pectin Core-Shell Beads Encapsulating Metformin–Clay Intercalation Compounds for Controlled Delivery. *New Journal of Chemistry*, **44**(24); 10102–10110
- Sabdon, A., N. Afiati, and H. Haeruddin (2021). Fucoxanthin Identification and Purification of Brown Algae Commonly Found in Lombok Island, Indonesia. *Biodiversitas Journal of Biological Diversity*, **22**(3); 1527–1534
- Safitri, E., Z. Omaira, N. Nazaruddin, I. Mustafa, S. Saleha, R. Idroes, B. Ginting, M. Iqhrammullah, S. Alva, and M. Paristiowati (2022). Fabrication of an Immobilized Polyelectrolyte Complex (PEC) Membrane from Pectin-Chitosan and Chromoionophore ETH 5294 for PH-Based Fish Freshness Monitoring. *Coatings*, **12**(1); 88
- Salama, A. H., H. Elmotasem, and A. A. Salama (2020). Nanotechnology Based Blended Chitosan-Pectin Hybrid for Safe and Efficient Consolidative Antiemetic and Neuro-Protective Effect of Meclizine Hydrochloride in Chemotherapy Induced Emesis. *International Journal of Pharmaceutics*, **584**(June); 119411
- Santos, V. P., N. S. Marques, P. C. Maia, M. A. B. d. Lima, L. d. O. Franco, and G. M. d. Campos Takaki (2020). Seafood Waste As Attractive Source of Chitin and Chitosan Production and Their Applications. *International Journal of Molecular Sciences*, **21**(12); 4290
- Sarma, S., S. Agarwal, P. Bhuyan, J. Hazarika, and M. Ganguly (2022). Resveratrol-Loaded Chitosan-Pectin Core-Shell Nanoparticles As Novel Drug Delivery Vehicle for Sustained Release and Improved Antioxidant Activities. *Royal Society Open Science*, **9**(2); 210784
- Singh, K., M. K. Paidi, A. Kulshrestha, P. Bharmoria, S. K. Mandal, and A. Kumar (2022). Deep Eutectic Solvents Based Biorefining of Value-Added Chemicals from the Diatom *Thalassiosira andamanica* at Room Temperature. *Separation and Purification Technology*, **298**(1); 121636
- Soukoulis, C. and T. Bohn (2018). A Comprehensive Overview on the Micro-and Nano-Technological Encapsulation Advances for Enhancing the Chemical Stability and Bioavailability of Carotenoids. *Critical Reviews in Food Science and Nutrition*, **58**(1); 1–36
- Sriamornsak, P. and C. R. Dass (2022). Chitosan Nanoparticles in Atherosclerosis—Development to Preclinical Testing. *Pharmaceutics*, **14**(5); 935
- Tian, L., A. Singh, and A. V. Singh (2020). Synthesis and Characterization of Pectin-Chitosan Conjugate for Biomedical Application. *International Journal of Biological Macromolecules*, **153**(June); 533–538
- Wang, H., Y. Zhang, L. Chen, W. Cheng, and T. Liu (2018). Combined Production of Fucoxanthin and Epa from Two Diatom Strains *Phaeodactylum tricornutum* and *Cylindrotheca fusiformis* Cultures. *Bioprocess and Biosystems Engineering*, **41**(April); 1061–1071
- Wang, Y., Q. Zhou, J. Zheng, H. Xiong, L. Zhao, Y. Xu, and C. Bai (2023). Fabricating Pectin and Chitosan Double Layer Coated Liposomes to Improve Physicochemical Stability of Beta-Carotene and Alter Its Gastrointestinal Fate. *International Journal of Biological Macromolecules*, **247**(August); 125780
- Xie, C., M. Huang, R. Ying, X. Wu, K. Hayat, L. K. Shaughnessy, and C. Tan (2023). Olive Pectin-Chitosan Nanocomplexes for Improving Stability and Bioavailability of Blueberry Anthocyanins. *Food Chemistry*, **417**(August); 135798
- Zhao, D., D. Yu, M. Kim, M. Y. Gu, S. M. Kim, C. H. Pan, G. H. Kim, and D. Chung (2019). Effects of Temperature, Light, and pH on the Stability of Fucoxanthin in an Oil-In-Water Emulsion. *Food Chemistry*, **291**(September); 87–93
- Zhao, X., X. Zhang, S. Tie, S. Hou, H. Wang, Y. Song, R. Rai, and M. Tan (2020). Facile Synthesis of Nano-Nanocarriers from Chitosan and Pectin with Improved Stability and Biocompatibility for Anthocyanins Delivery: An *In vitro* and *In vivo* Study. *Food Hydrocolloids*, **109**(December); 106114